

**Detecting  $z > 10$  objects  
through carbon, nitrogen and oxygen emission lines**

Maki Suginoara<sup>1,2</sup>, Tatsushi Suginoara<sup>1,3,4</sup>, and David N. Spergel<sup>5</sup>

Department of Astrophysical Sciences, Princeton University, Princeton, NJ 08544

**ABSTRACT**

By redshift of 10, star formation in the first objects should have produced considerable amounts of Carbon, Nitrogen and Oxygen. The submillimeter lines of C, N and O redshift into the millimeter and centimeter bands (0.5 mm–1.2 cm), where they may be detectable. High spectral resolution observations could potentially detect inhomogeneities in C, N and O emission, and see the first objects forming at high redshift. We calculate expected intensity fluctuations and discuss frequency and angular resolution required to detect them. For CII emission, we estimate the intensity using two independent methods: the line emission coefficient argument and the luminosity density argument. We find they are in good agreement. At  $1 + z \sim 10$ , the typical protogalaxy has a velocity dispersion of  $30 \text{ km s}^{-1}$  and angular size of 1 arcsecond. If CII is the dominant coolant, then we estimate a characteristic line strength of  $\sim 0.1 \text{ K km s}^{-1}$ . We also discuss other atomic lines and estimate their signal. Observations with angular resolution of  $10^{-3}$  can detect moderately nonlinear fluctuations of amplitude  $2 \cdot 10^{-5}$  times the microwave background. If the intensity fluctuations are detected, they will probe matter density inhomogeneity, chemical evolution and ionization history at high redshifts.

*Subject headings:* cosmology: theory — early universe — galaxies: formation — intergalactic medium — radio lines: general

submitted to *The Astrophysical Journal*

---

<sup>1</sup>Department of Physics, the University of Tokyo, Tokyo 113, Japan

<sup>2</sup>makis@astro.Princeton.EDU, JSPS Research Fellow

<sup>3</sup>RESCEU, School of Sciences, the University of Tokyo, Tokyo 113, Japan

<sup>4</sup>tatsushi@astro.Princeton.EDU, JSPS Postdoctoral Fellow

<sup>5</sup>dns@astro.Princeton.EDU

## 1. Introduction

When did the first stars and galaxies form? How can we detect them? Quasars were once the most distant objects that have ever been observed (Schneider, Schmidt and Gunn 1991). Now galaxies are beginning to take their place. Discovery of a large number of galaxies at  $z > 3$  (Steidel et al. 1996), and even up to  $z \sim 5$  (Franx et al. 1997, Dey et al. 1998), suggests that galaxies existed well before quasars did. In hierarchical models, star formation starts relatively early, by  $z \sim 30$  (Couchman and Rees 1986, Fukugita and Kawasaki 1994, Gnedin and Ostriker 1996, Tegmark et al. 1997), so even these  $z \sim 5$  galaxies are not representative of the first generation of objects.

The purpose of this paper is to investigate the possibility of detecting primordial objects through the atomic lines of carbon, nitrogen and oxygen, which should have been produced as a result of star formation. At low redshift, these submillimeter lines are important coolants (e. g., Bennett et al. 1994, Israel, White and Baas 1995, Stutzki et al. 1997, Young et al. 1997, Barvainis et al. 1997, Malhotra et al. 1997). If the source is at redshift  $1 + z \sim 10\text{--}20$ , the lines are redshifted to radio frequencies, where the atmosphere is more transparent and ground-based detectors with very high sensitivity and resolution exist.

If the source was uniformly distributed through space, then its emission would merely distort the spectrum. Since heavy elements produced by stars are distributed inhomogeneously, the observed emission should have intensity fluctuations as a function of both position and frequency. With high enough resolution one can in principle distinguish them from background. If we take  $1h^{-1}$  Mpc as a characteristic comoving scale of the inhomogeneity, this corresponds to  $\sim 1$  arcmin in angular scale, and  $\sim 10^{-3}$  in frequency resolution. On smaller scales, velocity dispersion of matter limits the scale that can be resolved in frequency space. In this paper we formulate the intensity fluctuations and estimate their magnitude. This signal should give us information on number density fluctuations of specific source elements at  $1 + z > 10$ . Detailed determination of the peak of this signal will also tell us at which epoch elements were ionized.

The rest of this paper is organized as follows. In the next section, we present our formalism for estimating the fluctuating signal. Then we estimate its magnitude in the case that the matter density fluctuations are calculated from the linear power spectrum in section 3. We also estimate optimal frequency and angular resolution for an object search. We focus on atomic line redshifted into present radio band, investigating carbon, nitrogen and oxygen emission lines at rest frame wavelength of hundreds of micrometers. In section 4, we discuss the size and the number density of nonlinear clumps at the reionization epoch, and estimate intensity from nonlinear clumps and the interval between enhance of intensity fluctuations. Section 5 gives discussion of merits and demerits as the signal of specific emission. After alternative estimation of CII luminosity in section 6, the final section gives our conclusion.

## 2. Observable intensity fluctuations

## 2.1. Formulation

Throughout this paper we make the following assumptions: by  $1 + z \sim 10\text{--}20$ , star formation has both formed metals and heated the surrounding gas initially to  $T \sim 10^4$  K. Cooling is compensated by heating so that the gas temperature  $T_{\text{gas}}$  is maintained much higher than the CMB temperature at that epoch but lower than  $\sim 10^4$  K. Cooling by atomic transitions exceeds Compton cooling, as we will see below.

Intensity  $I_\nu(z)$  of radiation in emitting medium at redshift  $z$  is obtained by solving the radiative transfer equation:

$$\frac{dI_\nu(z)}{dt} = cj_\nu(z) - 3H(z)I_\nu(z), \quad (1)$$

where  $c$  is the speed of light, and  $j_\nu(z)$  and  $H(z)$  denote the spontaneous emission coefficient and Hubble parameter, respectively. Differentiation with respect to time in the left hand side is taken with  $\nu(1+z)^{-1} = \text{const}$ . The second term in the right hand side comes from the effect of cosmic expansion. We have assumed that absorption is negligible. Integrating equation (1) yields the present intensity at frequency  $\nu_0$ :

$$I_{\nu_0}(z=0) = \int \frac{cj_\nu(z)}{(1+z)^3} dt = \int \frac{c}{H(z)(1+z)^4} j_\nu(z) dz, \quad (2)$$

where  $\nu = \nu_0(1+z)$  in the integrand. For spontaneous transition from an upper level  $u$  to a lower level  $l$  releasing a photon with energy  $h\nu_{\text{line}}$ , the emission coefficient is

$$j_\nu = \frac{h_P \nu_{\text{line}}}{4\pi} n_u A_{ul} \phi(\nu), \quad (3)$$

where  $h_P$  is the Planck constant,  $n_u$  is the number density of the source in the upper level,  $A_{ul}$  is the Einstein  $A$ -coefficient, and  $\phi(\nu) = \delta_D(\nu - \nu_{\text{line}})$  is the line profile function, which we take to be equal to delta function because both natural and thermal broadening is negligible for the expected frequency resolution. Since redshift of the source  $z_s$  is inferred from the relation:

$$1 + z_s = \frac{\nu_{\text{line}}}{\nu_0}, \quad (4)$$

we can express the line profile function as

$$\phi(\nu) = \phi(\nu_0(1+z)) = \frac{1+z_s}{\nu_{\text{line}}} \delta_D(z - z_s). \quad (5)$$

Using equations (3) and (5) in equation (2) yields intensity due to the line emission:

$$I_{\text{line}} = \frac{h_P c}{4\pi} A_{ul} n_u H^{-1}(z_s) (1+z_s)^{-3}. \quad (6)$$

In the Einstein–de Sitter universe, equation (6) reads

$$I_{\text{line}} = \frac{h_P c}{4\pi} H_0^{-1} A_{ul} f_u n_a (1+z_s)^{-9/2}, \quad (7)$$

where  $f_u = n_u/n_a$  is the fraction of the source that is in the upper state, and  $n_a$  is the local number density of the source.

## 2.2. Magnetic dipole transition

The spin–orbit interaction splits each spectroscopic term of an atom into a set of energy levels. Magnetic dipole transitions near the ground state of neutral and ionized carbon, nitrogen and oxygen have wavelength of hundreds of micrometers. We list such transitions in table 1 (Melnick 1988). These are candidates which produce intensity fluctuations.

## 2.3. Critical number density

We have seen the line intensity is proportional to the number density of the source that is in the upper state. Let us examine the condition for substantial number of the source to be in the upper state. If either spontaneous or stimulated emission occurs more rapidly than the collisional excitation by surrounding gas (mainly Hydrogen), very few atoms (or ions) will be in the upper state. The condition for collisional rate exceeding spontaneous and stimulated emission rates is

$$n_{\text{gas}} \geq n_{\text{gas}}^{\text{cr}}, \quad (8)$$

where  $n_{\text{gas}}^{\text{cr}}$  is the critical number density determined by

$$\gamma_{ul} n_{\text{gas}}^{\text{cr}} = A_{ul} \left[ 1 - \exp\left(-\frac{h\nu_{\text{line}}}{kT_{\text{CMB}}(z_s)}\right) \right]^{-1}, \quad (9)$$

with  $\gamma_{ul}$  being the rate coefficient for collisional de–excitation, and  $T_{\text{CMB}}(z)$  the CMB temperature at redshift  $z$ .

If  $n_{\text{gas}} > n_{\text{gas}}^{\text{cr}}$ , the excitation temperature of the source  $T_{\text{source}}$  is almost equal to  $T_{\text{gas}}$ , where  $T_{\text{gas}}$  is maintained around  $10^3$  K. In this case, the fraction  $f_u = f_u^{\text{eq}}$  does not depend on  $T_{\text{source}}$ . In CI case, the excitation energies of  $^3P_2$  and  $^1D$  levels correspond to 60K and  $1.5 \times 10^4$ K, respectively. If we assume that the gas is in thermal equilibrium at a temperature around  $10^3$ K, electrons in the  $(2p)^2$  shell of CI easily transit within  $^3P$  levels, while it is almost impossible to jump to  $^1D$  level. Therefore the fraction of atom that is in the state labeled as  $u$  is independent of matter temperature and determined by

$$f_u^{\text{eq}} \equiv \frac{n_u}{n_{\text{tot}}} = \frac{g_u}{\sum_{\text{same term}} g_i}, \quad (10)$$

where  $g_u = 2J + 1$  is the statistical weight of level  $u$ . Specifically, the fraction is 1/9, 3/9 and 5/9 for  $^3P_0, ^3P_1$  and  $^3P_2$  of neutral carbon.

If  $n_{\text{gas}} < n_{\text{gas}}^{\text{cr}}$ , the line intensity is diminished to

$$I_{\text{line}} \simeq I_{\text{line}}^{\text{eq}} \left( \frac{n}{n + n^{\text{cr}}} \right)_{\text{gas}}. \quad (11)$$

In CI (609  $\mu\text{m}$ ) case, the critical number density of Hydrogen is given by

$$n_{\text{H}}^{\text{cr}} = 73 \left( \frac{T_{\text{gas}}}{10^3 \text{ K}} \right)^{-0.34} \left[ 1 - \exp\left( -\frac{8.7}{1 + z_s} \right) \right]^{-1} \text{ cm}^{-3} \quad (12)$$

(Hollenbach and McKee 1989). The last factor in the above expression comes from the effect of stimulated emission. The effect is important for the CI 609  $\mu\text{m}$  line, but is negligible for the other fine structure transitions of interest here at  $1 + z_s \lesssim 20$ . The excitation of ions is induced mainly by the collisions with electrons, if the gas is ionized. The condition (8) is determined by the critical number density of electron

$$n_{\text{e}}^{\text{cr}} = 28 \left( \frac{T_{\text{gas}}}{10^3 \text{ K}} \right)^{0.50} \text{ cm}^{-3} \quad (13)$$

(Hollenbach and McKee 1989), in CII (158  $\mu\text{m}$ ) case.

## 2.4. Gas clumping

At  $1 + z \sim 10\text{--}20$ , the mean density of gas  $\simeq n_{\text{H}}^{\text{mean}} = 2 \times 10^{-4} [(1 + z)/10]^3 \text{ cm}^{-3}$  is lower than the critical number density. The condition for sufficient magnitude of signal, however, is attached to local number density of the source. The condition (8) can hold in the virialized object, even if  $n_{\text{gas}}^{\text{mean}} < n_{\text{gas}}^{\text{cr}}$ .

Let us express by  $F^{\text{cr}}$  the fraction of gas within the relevant scale which satisfies  $n_{\text{gas}} > n_{\text{gas}}^{\text{cr}}$ . Then the smoothed intensity is given by

$$\bar{I}_{\text{line}} = \frac{h_{\text{PC}}}{4\pi} H_0^{-1} A_{ul} f_u^{\text{eq}} F^{\text{cr}} \left[ \frac{n_{\text{a}}}{n_{\text{H}}} (z_s) \right] n_{\text{H},0} (1 + z_s)^{-3/2}, \quad (14)$$

where  $[n_{\text{a}}/n_{\text{H}}]$  is relative abundance of the atom, and  $n_{\text{H},0}$  is present Hydrogen number density. It is uncertain to what degree the baryonic gas condenses in dark matter halos. However, it seems reasonable to expect that the gas inside such halos can radiatively cool and form a gaseous disk, whose radius is  $\lambda r_{\text{vir}}$ , where  $\lambda$  is the spin parameter and  $r_{\text{vir}}$  is the virial radius (Peebles 1993, Dalcanton, Spergel and Summers 1997). If this is the case, we expect the mean gas density to be at least  $18\pi^2 \lambda^{-3}$  ( $\sim 10^6$ ) times the mean cosmic gas density at collapse, where  $\lambda = 0.05$  (Barnes and Efstathiou 1987) typically. For objects that form at  $1 + z > 10$ , this implies a characteristic number density of baryonic gas of at least  $300 \text{ cm}^{-3}$ . With this consideration in mind,  $F^{\text{cr}}$  is estimated by the fraction of matter within the collapsed objects with mass  $M$  greater than the Jeans mass  $M_{\text{J}}$ . By  $1 + z = 10$ , the fraction amounts to 50 percent of the total mass in the universe (Fukugita and Kawasaki 1994), assuming  $M_{\text{J}} \simeq 10^6 M_{\odot}$ . In the case that gas is considerably reheated,  $M_{\text{J}}$  rises to  $\simeq 10^8 M_{\odot}$  and  $F^{\text{cr}} = 0.3$  (Fukugita and Kawasaki 1994).

Gas clumps in these halos are optically thin in the relevant lines, and therefore the formulation in Section 2.1 is valid. For example, the one-dimensional velocity dispersion of a  $10^6 M_{\odot}$  halo

at  $1 + z = 10$  is estimated to be  $\sim 3 \text{ km s}^{-1}$  using the spherical collapse model. The size of the gas clump inside the halo with  $n_{\text{gas}} = 10^2 \text{ cm}^{-3}$  is  $\sim 10h^{-1} \text{ pc}$ . With these numbers and  $n_{\text{C}}/n_{\text{H}} = 0.01(n_{\text{C}}/n_{\text{H}})_{\odot}$ , the optical depth in the CI  $609 \mu\text{m}$  line is estimated to be around  $10^{-2}$ .

Intensity fluctuations with frequency correspond to number density fluctuations around relevant redshift:

$$\frac{\Delta I_{\text{line}}}{I_{\text{line}}} = \left( \frac{\Delta n}{n} \right)_{\text{source}}. \quad (15)$$

Even if the intensity  $I_{\text{line}}$  itself is smaller than the CMB intensity  $I_{\text{CMB}}$ , the fluctuations  $\Delta I_{\text{line}}/I_{\text{tot}} \cong \Delta I_{\text{line}}/I_{\text{CMB}}$  can be extracted as difference between those at different frequencies.

### 3. Intensity fluctuations due to linear perturbations

In this section, let us estimate the signal originated from the inhomogeneities on a characteristic scale  $\sim 1h^{-1} \text{ Mpc}$  corresponding to linear perturbation. In the next section, we focus on smaller scales and estimate the intensity from nonlinear clumps.

#### 3.1. Magnitude of the signal from carbon $609 \mu\text{m}$ emission

In this and next sections, we take CI ( $609 \mu\text{m}$ ) as an example (Yamamoto and Saito 1991). Essential discussion is common with other lines. Since the ionization state of the universe at  $z > 5$  is not known, we begin by assuming that most of the carbon at  $1 + z = 10$  is in the form of CI. The ratio of the intensity of CI ( $609 \mu\text{m}$ ) line emitted at  $1 + z = 10$  to total intensity  $I_{\text{tot}}$  can be calculated from equation (14) with  $f_u^{\text{eq}} = 1/3$  (Section 2.3):

$$\frac{\bar{I}_{\text{line}}}{I_{\text{tot}}} \cong \frac{\bar{I}_{\text{line}}}{I_{\text{CMB}}} \quad (16)$$

$$= 2 \times 10^{-6} \left( \frac{h}{0.5} \right)^{-1} \left( \frac{\Omega_{\text{B}} h^2}{0.025} \right) \left( \frac{n_{\text{C}}/n_{\text{H}}}{0.01(n_{\text{C}}/n_{\text{H}})_{\odot}} \right) \left( \frac{(n_{\text{C}}/n_{\text{H}})_{\odot}}{3.6 \times 10^{-4}} \right) \left( \frac{F^{\text{cr}}}{0.5} \right), \quad (17)$$

where  $h$  is the present Hubble parameter in units of  $100 \text{ km s}^{-1} \text{ Mpc}^{-1}$ , and  $\Omega_{\text{B}}$  is the present baryon density parameter. It is reasonable to expect that  $n_{\text{C}}/n_{\text{H}} = 0.01(n_{\text{C}}/n_{\text{H}})_{\odot}$  by  $1 + z = 10$ . Numerical simulation (Gnedin and Ostriker 1996) of nonlinear self-gravitating clumps at high redshift shows they have a metallicity  $Z = 0.03Z_{\odot}$  in the high density regions. Observation of CIV absorption in Ly  $\alpha$  forest clouds also supports the above value of  $n_{\text{C}}/n_{\text{H}}$ . In this paper, we adopt  $(n_{\text{C},\odot}, n_{\text{N},\odot}, n_{\text{O},\odot}) = (3.58, 1.12, 8.49) \times 10^{-4} n_{\text{H},\odot}$  for the solar abundance of carbon, nitrogen and oxygen (Anders and Grevesse 1989, Woosley and Weaver 1995).

For  $1 + z \lesssim 15$ , if most of the Carbon is in its ground states and  $n_{\text{gas}} > n_{\text{gas}}^{\text{cr}}$ , then cooling by the CI line emission exceeds Compton cooling: the cooling time due to the CI line emission can

be estimated as

$$t_{\text{cool}}^{\text{CI}} \sim \frac{(3/2)n_{\text{H}}k_{\text{B}}T_{\text{gas}}}{n_{\text{u}}h_{\text{P}}\nu_{\text{line}}A_{ul}} \sim 2 \times 10^7 \left( \frac{n_{\text{C}}/n_{\text{H}}}{0.01(n_{\text{C}}/n_{\text{H}})_{\odot}} \right)^{-1} \left( \frac{T_{\text{gas}}}{10^3 \text{K}} \right) \text{ yr}, \quad (18)$$

where  $k_{\text{B}}$  is Boltzmann’s constant. On the other hand, Compton cooling time is (Levin, Freese and Spergel 1992)

$$t_{\text{Compton}} \sim 1 \times 10^8 \left[ 1 + \left( \frac{n_{\text{e}}}{n_{\text{H}}} \right)^{-1} \right] \left( \frac{1+z}{10} \right)^{-4} \text{ yr}, \quad (19)$$

where  $n_{\text{e}}$  is the number density of free electrons.

We can estimate number density fluctuations in the standard cold dark matter (CDM) model with  $h = 0.5$ , the density parameter  $\Omega_0 = 1$ , and the present density fluctuations on  $8h^{-1}$  Mpc scale  $\sigma_8 = 1$ :

$$(\Delta n/n)_{\text{atom}} = \Delta M/M = 0.4 \quad (20)$$

on  $1h^{-1}$  Mpc scale at  $1+z = 10$ . This has been calculated from the CDM power spectrum  $P(k)$  given by Bardeen et al. (1986). This is a conservative estimate as the predicted fluctuation level is even larger in vacuum-dominated or open models. Therefore the magnitude of the signal becomes  $\Delta \bar{I}_{\text{line}}/I_{\text{CMB}} = 1 \times 10^{-6}$  in the standard CDM model. Table 1 summarizes predictions of intensity fluctuations with other elements. Note that each value has been calculated assuming that 100% of the element is in the form of the neutral atom or the ion in the first column. Actual signal is reduced by the fraction of the species in each element.

Since the metals are produced in dense regions, they will be ”biased” tracers of the underlying mass. This implies that

$$\left( \frac{\Delta n}{n} \right)_{\text{atom}} = b \left( \frac{\Delta M}{M} \right), \quad (21)$$

where  $b$  is the bias parameter. Gnedin and Ostriker (1996) find a strong correlation between metallicity and density. If  $Z \propto \rho^\alpha$ , then in the linear regime, this implies  $b = 1 + \alpha$ , which enhances the signal over the values estimated in table 1.

### 3.2. Characteristic fluctuation size

Now, we investigate the resolution that we need to detect the intensity fluctuations due to the line emission. The comoving length scale  $R_{\text{s}}$  probed with frequency resolution  $\Delta\nu/\nu$  is given by

$$R_{\text{s}} = c\Delta\eta = \frac{c(1+z)}{H(z)} \frac{\Delta a}{a} = \frac{c(1+z)}{H(z)} \frac{\Delta\nu}{\nu}, \quad (22)$$

where  $\eta$  is the conformal time, and  $a = (1+z)^{-1}$ . In the Einstein–de Sitter universe,

$$R_{\text{s}} = cH_0^{-1}(1+z)^{-1/2}\Delta\nu/\nu = 0.95 \left( \frac{1+z}{10} \right)^{-1/2} \left( \frac{\Delta\nu/\nu}{10^{-3}} \right) h^{-1} \text{ Mpc}. \quad (23)$$

An observation with a resolution  $\Delta\nu/\nu$  means that we probe the matter density inhomogeneities smoothed by spatial thickness  $R_s$ . Figure 1 shows predicted smoothed intensity fluctuations in the standard CDM model which are observed with given resolution  $\Delta\nu/\nu$  in CI (609  $\mu\text{m}$ ) and CI (370  $\mu\text{m}$ ) cases. It also shows the signal for CII (158  $\mu\text{m}$ ) in the case where most carbon is in the form of CII. Higher frequency resolution brings larger signal because of larger matter density fluctuations. For appropriate correspondence of frequency space to source positions,  $R_s$  is required to satisfy the relation:

$$\frac{\Delta\nu}{\nu}(R_s) > \frac{v_{\text{random}}(R_s; z)}{c}. \quad (24)$$

Here  $v_{\text{random}}(R_s; z)$  is the random velocity inside a spherical region of comoving radius  $R_s$ :

$$v_{\text{random}}(R_s; z) = \frac{a^2 \Omega^{0.6} H c}{2\pi^2} \int dk P(k) [1 - \bar{W}^2(R_s; k)], \quad (25)$$

where  $\bar{W}(R_s; k) \equiv 3(\sin kR_s - kR_s \cos kR_s)/(kR_s)^3$ . In the standard CDM model, the relation (24) yields  $\Delta\nu/\nu > 2 \times 10^{-5}$  and  $R_s > 0.02h^{-1}$  Mpc.

Let us move on to the needed angular resolution. To maximize observed intensity fluctuations, we need angular resolution  $\theta_{\text{res}}$  corresponding to  $R_s$ . In the Einstein–de Sitter universe, this angular resolution is given by

$$\theta_{\text{res}} = \frac{R_s}{\int da (a^2 H)^{-1}} = \frac{R_s}{2cH_0^{-1}(1 - 1/\sqrt{1+z})} \quad (26)$$

$$= \frac{\Delta\nu/\nu}{2(\sqrt{1+z} - 1)} = 0.79 \left( \frac{\Delta\nu/\nu}{10^{-3}} \right) \text{ arcmin}, \quad (27)$$

where the last value is for  $1+z=10$ .

#### 4. Intensity fluctuations due to nonlinear clumps

If we observe with high enough angular resolution, we should be able to detect features from individual clumps, rather than from linear matter inhomogeneities. More concentrated objects will be potentially stronger sources.

Hierarchical clustering model of structure formation in the universe tells us how nonlinear clumps formed in the process of gravitational instability growing. Let us estimate typical values of the comoving size of clumps  $R_{\text{typ}}$  and the mean separation among clumps  $\bar{R}_{\text{typ}}$  at  $1+z=10$ .

The comoving number density of clumps with in the mass range  $M \sim M + dM$  at  $z$  is given by the Press–Schechter (1974) formalism:

$$N(M, z)dM = \sqrt{\frac{2}{\pi}} \frac{\rho_0}{M} \frac{\delta_c}{D(z)} \left| \frac{1}{\sigma^2(M)} \frac{d\sigma(M)}{dM} \right| \exp \left[ -\frac{\delta_c^2}{2\sigma^2(M)D^2(z)} \right] dM, \quad (28)$$



where  $\rho_0$  is the mean comoving density of matter,  $\delta_c$  is the overdensity threshold,  $D(z)$  is the growing function of perturbations, and  $\sigma(M)$  is the variance of density field smoothed with mass scale  $M$ . Since  $\sigma(M)$  is a decreasing function of  $M$ , the comoving number density (equation 28) exponentially falls down at large mass. Therefore we can estimate the typical mass of clumps  $M_{\text{typ}}$  by a relation:

$$\sigma(M_{\text{typ}}) = \frac{1}{\sqrt{2}} \frac{\delta_c}{D(z_{\text{re}})}. \quad (29)$$

Since the density of virialized objects is  $18\pi^2$  times the mean density of the universe in spherical collapse model,  $R_{\text{typ}}$  is related to  $M_{\text{typ}}$  by  $R_{\text{typ}} = (3M_{\text{typ}}/4\pi\rho_0)^{1/3}(18\pi^2)^{-1/3}$ . Furthermore, the mean comoving separation  $\overline{R_{\text{typ}}} = n^{-1/3}$  is given from the comoving number density:

$$n(R_{\text{typ}}, z) = \int_{M_{\text{typ}}}^{\infty} N(M, z) dM. \quad (30)$$

We make use of the fitting formula for  $\sigma(M)$  in CDM models by (Kitayama and Suto 1996):

$$\sigma(M) \propto (1 + 2.208m^p - 0.7668m^{2p} + 0.7949m^{3p})^{-\frac{2}{9p}}, \quad (31)$$

which gives a good fit between  $10^{-7} < m < 10^5$ . Here  $p = 0.0873$ , and  $m \equiv M(\Omega_0 h^2)^2 / (10^{12} M_{\odot})$ . In the standard CDM model ( $\Omega_0 = 1$ ) with  $h = 0.5$  and  $\sigma_8 = 1$ , the above equations yield

$$R_{\text{typ}} = 0.015h^{-1} \text{ Mpc}, \quad \overline{R_{\text{typ}}} = 0.4h^{-1} \text{ Mpc}, \quad (32)$$

at  $1 + z = 10$ . In terms of  $\Delta\nu/\nu$ , these numbers correspond to  $2 \times 10^{-5}$  and  $4 \times 10^{-4}$ .

The one-dimensional velocity dispersion of these typical clumps is estimated as

$$v_{\text{typ}} = \sqrt{GM_{\text{typ}}(1+z)/(2R_{\text{typ}})} = 30 \text{ km s}^{-1}, \quad (33)$$

which corresponds to  $\Delta\nu/\nu = 1 \times 10^{-4}$ . Hence the effective overdensity of the clump is

$$\delta_{\text{eff}} = 18\pi^2 \times \frac{\Delta\nu}{\nu} (R_{\text{typ}}) / \frac{v_{\text{typ}}}{c} = 30. \quad (34)$$

In CI ( $609 \mu\text{m}$ ) case, for example, bumps of  $\Delta I/I_{\text{CMB}} = 1 \times 10^{-4}$  are expected to appear with mean interval of  $4 \times 10^{-4}$  in  $\Delta\nu/\nu$ , if observation is made with frequency resolution  $\Delta\nu/\nu = 1 \times 10^{-4}$  and angular resolution  $\theta_{\text{res}} \simeq 1$  arcsec. Here the angular resolution is related through equation (26) with the clump size  $R_{\text{typ}}$ . In more conventional units in radio astronomy, this line has intensity of  $\Delta T_{\text{line}} v_{\text{typ}} = 0.008 \text{ K km s}^{-1}$ , where  $\Delta T_{\text{line}}$  is the increment of brightness temperature. In CI ( $370 \mu\text{m}$ ) case, the amplitude of intensity fluctuations are estimated to be  $\Delta I/I_{\text{CMB}} = 4 \times 10^{-4}$ , that is  $\Delta T_{\text{line}} v_{\text{typ}} = 0.02 \text{ K km s}^{-1}$ , with the same resolution. Alternatively, if we assume that most carbon is in the form of CII, the signal of CII ( $158 \mu\text{m}$ ) line is estimated to be  $\Delta I/I_{\text{CMB}} = 3 \times 10^{-3}$ , that is  $\Delta T_{\text{line}} v_{\text{typ}} = 0.07 \text{ K km s}^{-1}$ .

## 5. Characteristics of individual lines

The observed signal will depend upon the ionization state and abundance of each element. Here, we present a simple consideration regarding the ionization state based on ionization potential. More realistic treatment of ionization of each element requires detailed computation including temperature and density inhomogeneities of gas and radiative transfer, which is beyond the scope of this paper.

CI 609  $\mu\text{m}$  and 370  $\mu\text{m}$  lines have the longest wavelength among the lines discussed here. If  $1 + z_s \sim 10\text{--}20$ , they are easiest to observe from ground. In addition, they can easily be distinguished from others. Even if the signal is weak, one can extract the signal by cross-correlating different portions of observed spectrum corresponding to these two wavelengths. The most serious concern is that the same star that produce carbon, will quickly ionize much of it to CII. The ionization potential of CI, 11.3 eV, is smaller than that of hydrogen, so we may have large mostly neutral regions containing CII.

Since carbon is so easily ionized, CII 158  $\mu\text{m}$  line may be a more promising candidate to be detected. CII is the brightest submillimeter line in our galaxy (Mizutani et al. 1994). Unfortunately, this is a single line and its higher frequency makes ground-based detection more challenging.

Other promising candidates are NII 204  $\mu\text{m}$  and 122  $\mu\text{m}$ , and OI 146  $\mu\text{m}$  lines. Nitrogen is expected to be abundant only after a relatively low redshift, since it is mainly produced in metal-enriched stars through incomplete CNO burning. Moreover, the ionization potential of nitrogen is 14.5 eV, so it is more difficult to ionize than hydrogen. On the other hand, OI abundance is supposed to peak around the reionization epoch; the ionization potential of oxygen is 13.6 eV, nearly equal to that of hydrogen, and charge exchange reaction ( $\text{O}^+ + \text{H} \leftrightarrow \text{O} + \text{H}^+$ ) imply that  $n_{\text{OI}}/n_{\text{OII}} \sim n_{\text{HI}}/n_{\text{HII}}$ .

The other, relatively short-wavelength lines are not likely to be observed from the ground, unless there was significant amount of metal production by  $1 + z \sim 25\text{--}50$ . Moreover, NIII and OIII probably never have been dominant species in each element; the ionization potential of NII and OII are 29.6 eV and 35.1 eV, respectively. However, their line intensity is so strong that they may be useful to place an interesting constraint on the state of matter and radiation field at  $1 + z \sim 25\text{--}50$ .

## 6. Alternative estimate of CII intensity

We can make an alternative estimate of the CII 158  $\mu\text{m}$  line intensity, clued by the measurement that roughly 1 percent of the luminosity from low redshift galaxies is emitted in the CII line (Malhotra et al. 1997). Though there is a possibility that the metal contamination may have somewhat changed the fraction, we assume that the same fraction (1 percent) of the

luminosity from small cloudlets at  $z = z_s$  is emitted in the CII line.

We estimate the luminosity density  $\mathcal{L}_{\text{CII}}$  of the CII emission instead of  $h_{\text{P}}\nu_{\text{line}}n_u A_{ul}$  in equation (3). We assume that the small cloudlets evolve with a constant star formation rate  $B^{\text{com}}$  per comoving unit volume from the Salpeter type initial mass function  $\phi(M)$  (Salpeter 1955) and achieve metallicity  $Z(z_s) = 0.01Z_{\odot}$  by  $z = z_s$ . We use the integrated abundance yields of type II supernovae tabulated by Thielemann, Nomoto, and Hashimoto (1993) to derive the star formation rate

$$B^{\text{com}} = 0.2 M_{\odot} \text{Mpc}^{-3} \text{yr}^{-1} \left( \frac{1+z_s}{10} \right)^{3/2} \left( \frac{h}{0.5} \right) \left( \frac{n_H^{\text{com}}}{2.1 \times 10^{-7} \text{cm}^{-3}} \right) \left( \frac{\rho_{\text{C},\odot}/\rho_{\text{H},\odot}}{0.0043} \right) \left( \frac{Z/Z_{\odot}}{0.01} \right), \quad (35)$$

where  $n_H^{\text{com}}$  is the comoving number density of hydrogen. Then the comoving luminosity density in the B-band is given by

$$\mathcal{L}_B^{\text{com}} = \int^{M_{\tau}} B^{\text{com}} t_u(z_s) \phi(M) L_B(M) dM + \int_{M_{\tau}} B^{\text{com}} \tau(M) \phi(M) L_B(M) dM, \quad (36)$$

where  $t_u(z_s)$  is the age of the universe at  $z = z_s$ ,  $\tau(M)$  and  $L_B(M)$  are the age and the B-band luminosity of a star whose mass is  $M$ , respectively, and  $M_{\tau}$  is the mass which satisfies  $\tau(M_{\tau}) = t_u(z_s)$ .

The resultant comoving luminosity density is  $\mathcal{L}_{\text{CII}}^{\text{com}} = 0.01\mathcal{L}_B^{\text{com}} = 4 \times 10^7 L_{\odot} \text{Mpc}^{-3}$  (at  $1+z_s = 10$ ),  $7 \times 10^7 L_{\odot} \text{Mpc}^{-3}$  (at  $1+z_s = 20$ ). We find that these are in good agreement with the previous estimate  $h_{\text{P}}\nu_{\text{line}}\bar{n}_u^{\text{com}} A_{ul} = 6 \times 10^7 L_{\odot} \text{Mpc}^{-3}$ . We conclude that the CII intensity fluctuations estimated alternatively here are almost the same magnitude as the previous result (table 1).

## 7. Conclusion

We have proposed a new and promising method to detect the first objects: search for carbon, nitrogen and oxygen line emission at  $1+z = 10\text{--}20$ . We conclude that the intensity fluctuations originated from the emission are detectable in radio band (0.5 mm–1.2 cm). If observation is carried out with angular resolution  $\theta_{\text{res}} = 1$  arcmin and spectral resolution  $\Delta\nu/\nu = 10^{-3}$ , the magnitude of the smoothed intensity fluctuations corresponding with linear matter density fluctuations is predicted as  $\Delta\bar{I}_{\text{line}}/I_{\text{tot}} = (1 \text{ and } 3) \times 10^{-6}$  (in CI 609 and 370  $\mu\text{m}$  cases) from sources at  $1+z = 10$ , in the standard CDM model. The predictions for other lines are  $\Delta\bar{I}_{\text{line}}/I_{\text{tot}} = (20, 70, 3, 20) \times 10^{-6}$ , respectively, in [158(CII), 146(OI), 204(NII), 122(NII)]  $\mu\text{m}$  cases.

Observation with  $\theta_{\text{res}} = 1$  arcsec and  $\Delta\nu/\nu = 10^{-4}$  resolve individual protogalaxies with velocity dispersion of  $30 \text{ km s}^{-1}$ . We predict line intensities relative to the microwave background of  $\Delta I_{\text{line}}/I_{\text{tot}} = (1, 4, 30, 80, 4, 30) \times 10^{-4}$  or equivalently  $\Delta T_{\text{line}} v_{\text{typ}} = (0.8, 2, 7, 20, 1, 6) \times 10^{-2} \text{ K km s}^{-1}$  for [609(CI), 370(CI), 158(CII), 146(OI), 204(NII), 122(NII)]  $\mu\text{m}$  lines, respectively. If detected,

these features will provide useful information on matter inhomogeneities at  $1 + z = 10\text{--}20$ . They will also probe chemical evolution and reionization time  $z_{\text{re}}$  itself.

We thank John H. Black, Bruce T. Draine, Thomas Herbig, Ryoichi Nishi, Jeremiah P. Ostriker, Lyman A. Page, Suzanne T. Staggs, and Hajime Susa for useful discussion. DNS acknowledges the MAP/MIDEX project for support. MS and TS acknowledge support from Research Fellowships of the Japan Society for the Promotion of Science.

## REFERENCES

- Anders, E., and Grevesse, N. 1989, *Geochim. Cosmochim. Acta*, 53, 197
- Bardeen, J. M., Bond, J. R., Kaiser, N., and Szalay, A. S. 1986, *ApJ*, 304, 15
- Barnes, J., and Efstathiou, G. 1987, *ApJ*, 319, 575
- Barvainis, R., Maloney, P., Antonucci, R., and Alloin, D. 1997, *ApJ*, 484, 695
- Bennett, C. L., et al. 1994, *ApJ*, 434, 587
- Couchman, H. M. P., and Rees, M. J. 1986, *MNRAS*, 221, 53
- Dalcanton, J. J., Spergel, D. N., and Summers, F. J. 1997, *ApJ*, 482, 659
- Dey, A., et al. 1998, *ApJ Letters*, in press (astro-ph/9803137)
- Franx, M., Illingworth, G. D., Kelson, D. D., van Dokkum, P. G., and Tran, K.-V. 1997, *ApJ*, 486, L75
- Fukugita, M., and Kawasaki, M. 1994, *MNRAS*, 269, 563
- Gnedin, N. Y., and Ostriker, J. P. 1997, *ApJ*, 486, 581
- Hollenbach, D., and McKee, C. F. 1989, *ApJ*, 342, 306
- Israel, F. P., White, G. J., and Baas, F. 1995, *A&A*, 302, 343
- Kitayama, T., and Suto, Y. 1996, *ApJ*, 469, 480
- Levin, J. J., Freese, K., and Spergel, D. N. 1992, *ApJ*, 389, 464
- Malhotra, S., et al. 1997, *ApJ*, 491, L27
- Melnick, G. J. 1988, *International Journal of Infrared and Millimeter Waves*
- Mizutani, K., et al. 1994, *ApJS*, 91, 613

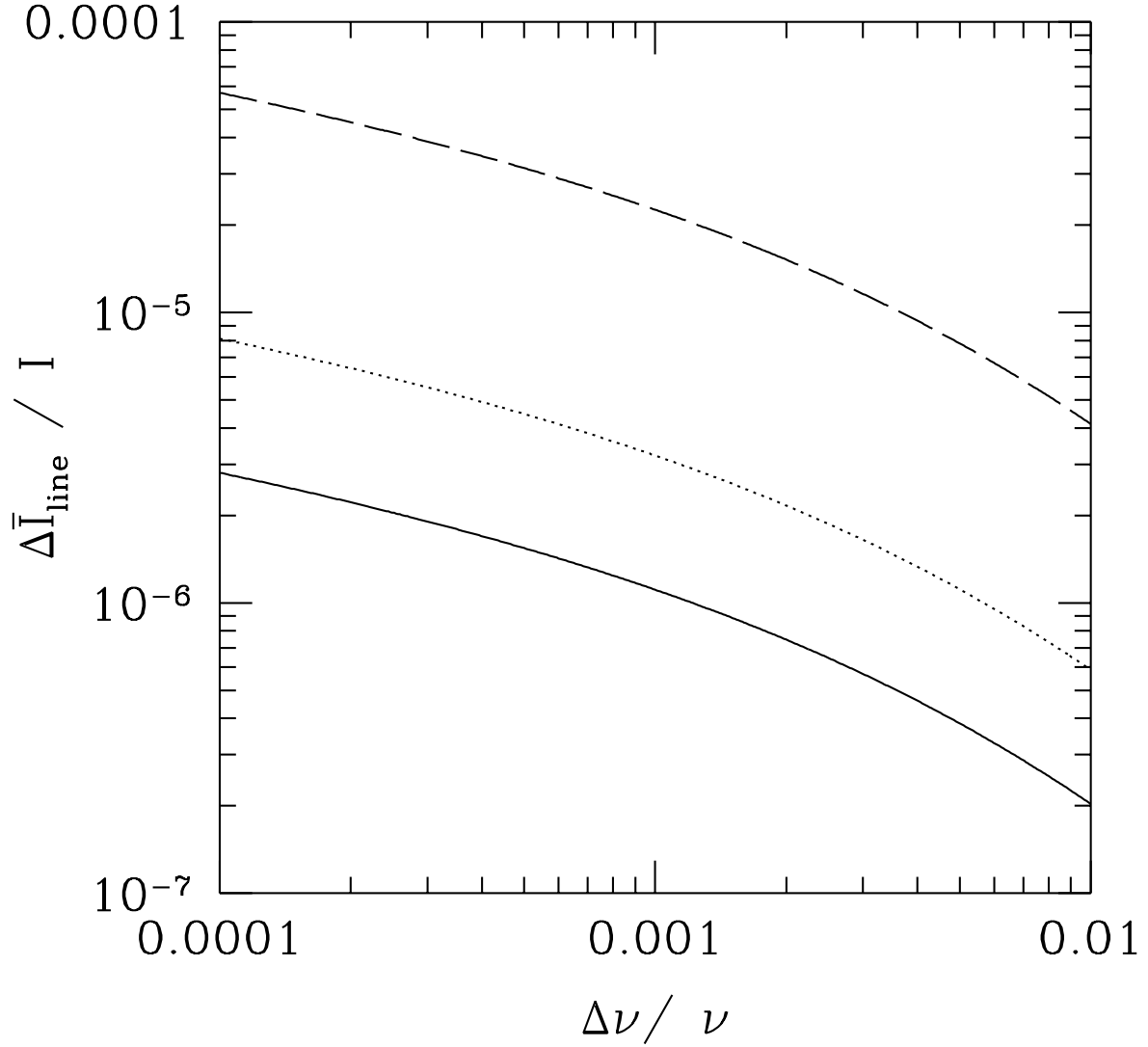


Fig. 1.— Smoothed intensity fluctuations: Solid and Dotted lines show the signals for CI (609  $\mu\text{m}$ ) and CI (370  $\mu\text{m}$ ) emission, respectively, if most of the carbon is in the form of CI. Broken line shows the signal for CII (158  $\mu\text{m}$ ) emission in the case where CII ion state is preferred.

- Peebles, P. J. E. 1993, *Principles of Physical Cosmology*: Princeton Univ. Press
- Press, W. H., and Schechter, P. 1974, *ApJ*, 187, 425
- Salpeter, E., E. 1955, *ApJ*, 121, 161
- Schneider, D. P., Schmidt, M., and Gunn, J. E. 1991, *AJ*, 102, 837
- Steidel, C. C., Giavalisco, M., Pettini, M., Dickinson, M., and Adelberger, K. L., 1996, *ApJ*, 462, L17
- Stutzki, J., et al. 1997, *ApJ*, 477, L33
- Tegmark, M., Silk, J., Rees, M. J., Blanchard, A., Abel, T., and Palla, F. 1997, *ApJ*, 474, 1
- Thielemann, F.-K., Nomoto, K., and Hashimoto M. 1993, *Origin and Evolution of the Elements*, N. Prantzos, E. Vangioni–flam and M. Cassè: Cambridge, 297
- Woosley, S. E., and Weaver, T. A. 1995, *ApJS*, 101, 181
- Yamamoto, S., and Saito, S. 1991, *ApJ*, 370, L103
- Young, K., Cox, P., Huggins, P. J., Forveille, T., and Bachiller, R. 1997, *ApJ*, 482, L101

Table 1: Transition lines and intensity fluctuations: the estimates of  $\Delta\bar{I}_{\text{line}}/I_{\text{tot}}$  assume that the each ion is the preferred ionization state.

Species	Transition	Wavelength ( $\mu\text{m}$ )	$A_{ul}$ ( $\text{s}^{-1}$ )	$\Delta\bar{I}_{\text{line}}/I_{\text{tot}}$
C <sup>0</sup>	${}^3P_1 \rightarrow {}^3P_0$	609	$7.93 \times 10^{-8}$	$1 \times 10^{-6}$
C <sup>0</sup>	${}^3P_2 \rightarrow {}^3P_1$	370	$2.68 \times 10^{-7}$	$3 \times 10^{-6}$
C <sup>+</sup>	${}^2P_{3/2} \rightarrow {}^2P_{1/2}$	158	$2.36 \times 10^{-6}$	$2 \times 10^{-5}$
N <sup>+</sup>	${}^3P_1 \rightarrow {}^3P_0$	204	$2.13 \times 10^{-6}$	$3 \times 10^{-6}$
N <sup>+</sup>	${}^3P_2 \rightarrow {}^3P_1$	122	$7.48 \times 10^{-6}$	$2 \times 10^{-5}$
N <sup>++</sup>	${}^2P_{3/2} \rightarrow {}^2P_{1/2}$	57.3	$4.77 \times 10^{-5}$	$2 \times 10^{-3}$
O <sup>0</sup>	${}^3P_1 \rightarrow {}^3P_2$	63.2	$8.95 \times 10^{-5}$	$9 \times 10^{-3}$
O <sup>0</sup>	${}^3P_0 \rightarrow {}^3P_1$	146	$1.70 \times 10^{-5}$	$7 \times 10^{-5}$
O <sup>++</sup>	${}^3P_2 \rightarrow {}^3P_1$	51.8	$9.75 \times 10^{-5}$	$5 \times 10^{-2}$
O <sup>++</sup>	${}^3P_1 \rightarrow {}^3P_0$	88.4	$2.62 \times 10^{-5}$	$7 \times 10^{-4}$